UNCLASSIFIED

CONTRACT NO. NONR 839(23)
PROJECT NO. NR 064-433

ABLATION OF A HOLLOW SPHERE

by

Richard F. Parisse and Jerome M. Klosner

POLYTECHNIC INSTITUTE OF BROOKLYN

DEPARTMENT
of
AEROSPACE ENGINEERING
and
APPLIED MECHANICS

AUGUST 1963

PIBAL REPORT NO. 670

Contract No. Nonr 839(23)
Project No. NR 064-433

ABLATION OF A HOLLOW SPHERE

by

Richard F. Parisse and Jerome M. Klosner

Polytechnic Institute of Brooklyn

Department of

Aerospace Engineering and Applied Mechanics

August 1963

PIBAL Report No. 670

Abstract

The ablation characteristics of a thick walled spherical shell considering radial heat flow is investigated. The outer surface of the shell is subjected to a time-dependent, point-symmetric, radial heat input and the inner surface is insulated. The melted material is assumed to be immediately removed upon formation.

Two approximate solutions to the problem are developed and compared. The first method is an adoption of Citron's solution [1]* which is based on the assumption that the temperature distribution through the thickness of the body may be expressed in a Taylor series expansion about the melting surface at any time. The second method employs the heat balance technique suggested by Goodman [2] which satisfies the heat conduction equation on the average.

Numerical calculations are performed for an aluminum sphere having a 7-3/4 inch outside diameter and a one-inch wall thickness, subjected to a constant heat flux. Constant thermal properties are assumed for these calculations.

---

*Numbers inside the square brackets refer to the References.

Symbols

a	initial outside radius of spherical shell
b	inside radius of spherical shell
B^*	non-dimensional parameter; $\frac{k(T_m)[T_m - T_i]}{Q_o[a - b]}$
$c(T)$	specific heat of material, a function of temperature
$\bar{c}$	non-dimensional specific heat parameter; $\frac{c(T)}{c(T_m)}$
G	temperature integral; $\int_b^{r_s} u\, dr$
h	surface heat transfer coefficient
$k(T)$	thermal conductivity of material, a function of temperature
$\bar{k}$	non-dimensional thermal conductivity parameter; $\frac{k(T)}{k(T_m)}$
L	latent heat of fusion
M^*	non-dimensional parameter; $\frac{c(T_m)[T_m - T_i]}{L}$
$Q(t)$	heat flux on the outer surface of body [for aerodynamic heating $Q(t) = h(T_s - T_w)$]
$\bar{Q}$	non-dimensional heat flux parameter; $\frac{Q(t)}{Q_o}$
Q_o	heat flux at $t = t_m$
r	radial distance
$r_s(t)$	outside radius of the spherical shell at any time
R_s	non-dimensional outside radius parameter; $\frac{a - r_s}{a - b}$
t	time
t_m	melt time, time at which the melting temperature is first reached on the outside surface $(r = a)$
$T(r,t)$	temperature $(t \geq t_m)$
$T_o(r,t)$	pre-melt temperature $(t \leq t_m)$

T_i	constant initial temperature of the body
T_m	melting temperature of the material
T_s	stagnation temperature of the external flow field
T_w	outside surface temperature [for $t \geq t_m$, $T_w \equiv T_m$]
$u(r,t)$	temperature transformation; $u = Tr (u_o = T_o r)$
Z	non-dimensional space transformation; $r - b/r_s - b$
$\theta(Z,\tau)$	non-dimensional temperature parameter; $T - T_i/T_m - T_i$
α_o	non-dimensional surface heat transfer coefficient [$\alpha_o = ha/k$]
κ	thermal diffusivity; $k/\rho c$
ρ	density
τ	non-dimensional time parameter; $\dfrac{\kappa(T_m)[t - t_m]}{(a - b)^2}$

Introduction

Upon re-entry the extremely high heat inputs have major effects on the structural integrity of the space vehicle. The heat inputs are of such magnitude that the melting temperature of the space vehicle may be reached on the outside surface. Melting of the surface will then occur, and the aerodynamic shearing forces will tend to remove this molten material from the original structure. This destructive process, which is generally termed ablation, has been used quite successfully for beneficial purposes, such as the heat shield design. This technique employs coating the space vehicle with a shielding material. During re-entry the ablation of this shielding material absorbs a great percentage of the heat input to the entire body and thereby protects the load-carrying structure and interior of the vehicle from heat damage. It is of importance to the designer to obtain an accurate prediction of the amount of shielding material needed to absorb a given heat input and to determine the corresponding temperatures and thermal stresses within the shield and back-up structure.

The treatment of any problem in heat conduction involving more than one space variable is a complicated procedure. With the inclusion of ablation of the outside surface, the problem becomes non-linear, even in the simplest cases. For this reason, all the available literature investigated treated problems in one space variable.

The basic modern work on ablation was carried outin 1948 by Landau [3] in which he set up the equations and boundary conditions for ablation of a finite and semi-infinite slab and carried out the solution for the semi-infinite slab under constant heat input and thermal properties with the use of computing machinery.

It was assumed that the melted material was immediately removed upon formation.

Lotkin [4] developed a numerical procedure for the solution of an ablating finite slab. Immediate removal of the melt was assumed, as were a time-dependent heat flux, and temperature-dependent thermal properties. Again high speed computing machines were essential to the solution of the problem.

A computer technique for the solution of the slab problem under a time-dependent heat input was developed by Ehrlich [5]. In this case, however, the melted material was assumed to remain in contact with the original body, necessitating satisfying the heat conduction equation in both the melted and unmelted material.

Dewey, Schlesinger and Sashkin [6] developed a numerical solution for a cylinder of finite thickness under radial heat input with one moving boundary and variable thermal conductivity. A simple mathematical model for aerodynamic ablation was developed by Goodman [7], and Adams [8] discussed the important ablation parameters and the various solutions which have been obtained, and compared these to experimental results. Excellent background material for the entire heat conduction problem as well as some specific solutions related to changes of phase can be found in Carslaw and Jaeger [9].

In an attempt to arrive at solutions of the ablation problem without the use of high-speed computing machinery, a few approximate techniques have been developed. Goodman [2] employed the heat balance technique for the solution, in closed, analytical form, of the ablating semi-infinite slab and compared these results with Landau's exact solution. Citron [1,10] developed two techniques for the solution of the finite slab. One method [1] was based on the assumption that the temperature distribution through the thickness of the slab could be expressed in a Taylor series expansion in space about the melting surface. This yielded an ordinary, non-linear, differential equation in terms of the melt depth as a function of time. The solution, which must be obtained numerically, could be readily computed on a desk calculator. Citron's second method [10] consisted of reducing the non-linear, partial differential equation into two ordinary differential equations, one linear and one non-linear, in terms of a temperature function and the melt depth. The solution could be obtained by successive approximations utilizing a desk calculator. Boley [11] considered still another procedure for the slab with immediate removal of the melt and constant thermal properties. An ordinary integro-differential problem which can be solved numerically or in series form for the exact solution of the melting problem was developed. A solution for the semi-infinite slab under constant heat input was obtained.

Interaction of the ablating material with the external flow field was also considered by certain investigators. When a material ablates, the molten material, or the vaporized material in the case of a subliming solid, or a mixture of vapor and liquid, is injected from the body into the surroundings of the body. In the case of re-entry, the injection is made into the boundary layer and this produces the added beneficial effect of reducing the heat input to the body. Swann and South [12], Lew and Fanucci [13], Fleddermann and Hurwicz [14], and Sutton [15], include investigations of such phenomena. In Ref. [16], Economos includes this factor in calculating ablation of semi-infinite slabs of plastic materials, such as Lucite, and compares the results with experimental data.

In this report, an attempt has been made to determine the solution of the ablation problem for a thick walled hollow sphere, using the Goodman [2] and Citron [1] techniques.

The two methods have been compared in an attempt to evaluate the inherent attributes of each and to determine, if possible, which method is more practical in actual application. It was assumed that the outer surface of the sphere was subjected to a prescribed point-symmetric, time-dependent, radial heat flux and that the inner surface of the sphere was insulated. The initial temperature distribution in the body was constant and lower than the melting temperature of the material. Thermal properties were considered to be functions of temperature (for the Citron method) and it was also assumed that the melted material was immediately removed upon formation.

Numerical calculations of melt depth and temperature distributions as functions of time were carried out for an aluminum sphere of 1" wall thickness and 7-3/4" outside diameter under aerodynamic heat inputs corresponding to hypersonic flow. Material properties were assumed constant for these calculations.

Theoretical Analysis

The problem treated is the ablation of a hollow sphere initially at a uniform temperature (T_i) which is lower than the melt temperature. It is assumed that the outer surface ($r = a$) is subjected to a time-dependent, point-symmetric, radial heat input $Q(t)$, that the inner surface ($r = b$) is insulated, and that the material has temperature-dependent thermal properties. The molten material is assumed to be immediately removed so that the outer boundary of the body is always considered to be at the melt temperature.

The overall analysis can be divided into two separate investigations: i) the pre-melt analysis, and ii) the melt analysis.

i) Pre-melt Analysis:

This analysis covers the time interval between the initial time ($t = 0$), when the body is at a constant initial temperature (T_i), and the melt time ($t = t_m$), the time at which the melting temperature (T_m) of the material is first reached at the heated surface. Attainment of this solution is necessary for the melt analysis, for in order to continue the solution of the problem once melting begins it is necessary to know the time (t_m) when melting starts and the temperature distribution through the thickness of the body at this time.

Before melt temperature is reached on the outer surface of the hollow sphere, the heat conduction equation is:

$$\rho c \frac{\partial T_o}{\partial t} = \frac{1}{r^2}\frac{\partial}{\partial r}\left(k r^2 \frac{\partial T_o}{\partial r}\right) \quad ; \quad b < r < a \qquad (1)$$

under the conditions:

$$\text{a)}\quad T_o(r,0) = T_i$$

$$\text{b)}\quad Q(t) = k\left(\frac{\partial T_o}{\partial r}\right)_{a,t}$$

$$\text{c)}\quad \left(\frac{\partial T_o}{\partial r}\right)_{b,t} = 0 \qquad (2)$$

Many solutions of the pre-melt problem exist (see, e.g., Refs. [9] and [17]), and thus in general the melt time and the corresponding temperature distribution can be readily obtained.

ii) Melt Analysis:

When melting begins it is assumed that the outer surface of the sphere always remains at the melt temperature and that the melt is immediately removed. The total heat input to the body is now divided into two parts. One portion enters the solid while the other accounts for the latent heat of fusion absorbed in the ablation process.

The heat conduction equation is:

$$\rho c \frac{\partial T}{\partial t} = \frac{1}{r^2}\frac{\partial}{\partial r}\left(kr^2\frac{\partial T}{\partial r}\right) \quad ; \quad b < r < r_s(t) \qquad (3)$$

where $r_s(t)$ is the varying outside radius of the sphere.

The conditions are:

$$\begin{aligned}
&a) \quad T(r,t_m) = T_o(r,t_m) \\
&b) \quad T(r_s,t) = T_m \\
&c) \quad Q(t) = k(T_m)\left(\frac{\partial T}{\partial r}\right)_{r_s,t} - \rho L \frac{dr_s}{dt} \\
&d) \quad \left(\frac{\partial T}{\partial r}\right)_{b,t} = 0 \\
&e) \quad r_s(t_m) = a
\end{aligned} \qquad (4)$$

An auxiliary condition can be imposed from a consideration of continuity of heat input at time $t = t_m$. From the pre-melt analysis the boundary condition on the heat input at $t = t_m$ from Eq. (2b) is:

$$Q(t_m) = k(T_m)\left(\frac{\partial T_o}{\partial r}\right)_{a,t_m}$$

and from the melt analysis the Boundary Condition from Eq. (4c) is:

$$Q(t_m) = k(T_m)\left(\frac{\partial T}{\partial r}\right)_{r_s(t_m),t_m} - \rho L \left(\frac{dr_s}{dt}\right)_{t_m} .$$

Now, since $r_s(t_m) \equiv a$, and $T(r,t_m) = T_o(r,t_m)$, then for continuity:

$$\left(\frac{dr_s}{dt}\right)_{t_m} \equiv 0 \qquad (5)$$

The solution of the problem, described by Eqs. (3), (4), and (5), will now be treated by two different approximate numerical techniques.

Method I:

In this approach, the technique utilized by Citron [1] for a slab is applied to the spherical shell. Material properties are assumed to be functions of temperature. The method consists of applying a transformation which allows the consideration of a body of constant unit thickness at all times in lieu of a body of varying thickness, and then expressing the temperature distribution at any time in this unit body by a Taylor series expansion in space about the melting surface.

For the spherical shell the transformation used is

$$Z = \frac{r - b}{r_s - b} \tag{6}$$

so that at $r = r_s$, $Z = 1$

and at $r = b$, $Z = 0$.

Using this transformation along with the following non-dimensional parameters

$$\tau = \frac{\kappa(T_m)(t - t_m)}{(a - b)^2} \quad ; \quad R_s(\tau) = \frac{a - r_s}{a - b}$$

$$\theta(Z,\tau) = \frac{T - T_i}{T_m - T_i} \quad ; \quad \bar{Q}(\tau) = \frac{Q(t)}{Q_o} \tag{7}$$

$$\bar{k} = \frac{k(T)}{k(T_m)} \quad ; \quad \bar{c} = \frac{c(T)}{c(T_m)}$$

where Q_o is the heat input at t_m. The heat conduction Equation (3) becomes

$$\frac{\partial^2\theta}{\partial Z^2} = \frac{\bar{c}}{\bar{k}}(1-R_s)^2\frac{\partial\theta}{\partial\tau} + \frac{\bar{c}}{\bar{k}}Z(1-R_s)\dot{R}_s\frac{\partial\theta}{\partial Z} - \frac{2(1-R_s)}{(1-R_s)Z + \frac{b/a}{1-b/a}}\frac{\partial\theta}{\partial Z} - \frac{1}{\bar{k}}\frac{d\bar{k}}{d\theta}\left(\frac{\partial\theta}{\partial Z}\right)^2 \quad (8)$$

where $(\dot{\ })$ denotes differentiation with respect to τ, and the conditions (4a to 4e) become

a) $\theta(Z,\tau) = \theta_o(Z,\tau)$ at $\tau = 0$

b) $\theta(Z,\tau) = 1$ at $Z = 1$

c) $\left(\frac{\partial\theta}{\partial Z}\right)_{1,\tau} = (1-R_s)\left[\frac{\bar{Q}}{B^*} - \frac{\dot{R}_s}{M^*}\right]$ (9)

d) $\left(\frac{\partial\theta}{\partial Z}\right)_{o,\tau} = 0$

e) $R_s(0) = 0$

while Eq. (5), $\left(\frac{dr_s}{dt}\right)_{t_m} = 0$, becomes $\dot{R}_s(0) = 0$

and

$$B^* = \frac{k(T_m)[T_m - T_i]}{Q_o[a-b]}$$

$$M^* = \frac{c(T_m)[T_m - T_i]}{L}$$

It is now assumed that $\theta(Z,\tau)$ can be expressed as a Taylor series expansion in space about the melting face $Z=1$. That is,

$$\theta(Z,\tau) = \theta(1,\tau) + \left(\frac{\partial\theta}{\partial Z}\right)_{1,\tau}(Z-1) + \left(\frac{\partial^2\theta}{\partial Z^2}\right)_{1,\tau}\frac{(Z-1)^2}{2!} + \ldots. \quad (10)$$

The first term and the coefficient of the second term are known from conditions (9b and 9c)

$$\theta(1,\tau) = 1$$

$$\left(\frac{\partial\theta}{\partial Z}\right)_{1,\tau} = (1-R_s)\left[\frac{\bar{Q}}{B^*} - \frac{\dot{R}_s}{M^*}\right]$$

The coefficient of the third term can readily be found by evaluating Eq. (8) at $Z=1$. The result is

$$\left(\frac{\partial^2\theta}{\partial Z^2}\right)_{1,\tau} = (1-R_s)^2\left\{\left[\frac{\bar{Q}}{B^*} - \frac{\dot{R}_s}{M^*}\right]\left[\dot{R}_s - \frac{2}{1-R_s+\frac{b/a}{1-b/a}}\right] - \left[\frac{\bar{Q}}{B^*} - \frac{\dot{R}_s}{M^*}\right]^2\left(\frac{d\bar{k}}{d\theta}\right)_{1,\tau}\right\}$$

By successively differentiating Eq. (8) with respect to Z, $\frac{\partial^3\theta}{\partial Z^3}, \frac{\partial^4\theta}{\partial Z^4}, \ldots, \frac{\partial^n\theta}{\partial Z^n}$, can be obtained and these can be evaluated at $(1,\tau)$ to form the remaining $n-2$ coefficients of the Taylor series expansion. The result is that an expression for $\theta(Z,\tau)$ is obtained containing Z and R_s and its first K derivatives when 2K or 2K + 1 terms of the Taylor series are included.

Now if condition (9d), which is

$$\left(\frac{\partial\theta}{\partial Z}\right)_{0,\tau} = 0$$

is applied to Eq. (10), then

$$0 = \left(\frac{\partial\theta}{\partial Z}\right)_{1,\tau} - \left(\frac{\partial^2\theta}{\partial Z^2}\right)_{1,\tau} + \frac{1}{2!}\left(\frac{\partial^3\theta}{\partial Z^3}\right)_{1,\tau} - \cdots\cdots \qquad (11)$$

and since $(\frac{\partial\theta}{\partial Z})_{1,\tau}$; $(\frac{\partial^2\theta}{\partial Z^2})_{1,\tau}$; .... ; $(\frac{\partial^n\theta}{\partial Z^n})_{1,\tau}$ have all been expressed in terms of R_s, $\dot{R}_s$, etc., the final result is that a non-linear, ordinary differential equation involving R_s and its derivatives alone has been obtained. It should be noted that this equation will always be linear in the highest order derivative term (when more than three terms are used in the expansion).

The series expansion of the temperature is terminated after 2K or 2K + 1 terms, thus leading to a differential equation of K^{th} order. Thus in addition to the initial conditions $R_s(0) = 0$, and $\dot{R}_s(0) = 0$, it is required to obtain K - 2 additional conditions. These K - 2 values, $\ddot{R}_s(0)$, $\dddot{R}_s(0)$ ...., $\overset{K-1}{R}_s(0)$ are obtained by matching the initial temperature distribution $\theta_o(Z,0)$ at K - 2 points.

The following numerical procedure can be used for the solution of the differential equation. For small τ, $R_s(\tau)$ can be expanded in a Taylor series about $\tau = 0$:

$$R_s(\tau) = R_s(0) + \dot{R}_s(0)\tau + \ddot{R}_s(0)\frac{\tau^2}{2!} + \dddot{R}_s(0)\frac{\tau^3}{3!} + \ldots.$$

where $\overset{K}{R}_s(0)$ is obtained by satisfying Eq. (11).

This can then be used to determine $R_s(\tau_1)$, $\dot{R}_s(\tau_1)$, ... $\overset{K-1}{R}_s(\tau_1)$ while Eq. (11) can then be used to determine $\overset{K}{R}_s(\tau_1)$. The numerical scheme then proceeds as follows:

$$R_s(\tau_i + \Delta\tau) = R_s(\tau_i) + \Delta\tau\,\dot{R}_s(\tau_i)$$
$$\dot{R}_s(\tau_i + \Delta\tau) = \dot{R}_s(\tau_i) + \Delta\tau\,\ddot{R}_s(\tau_i)$$
$$\vdots$$
$$\overset{K-1}{R}_s(\tau_i + \Delta\tau) = \overset{K-1}{R}(\tau_i) + \Delta\tau\,\overset{K}{R}_s(\tau_i)$$

and finally $\overset{K}{R}_s(\tau_i + \Delta\tau)$ can again be evaluated from Eq. (11). This procedure is continued until the entire solution is determined.

Method II:

A thorough investigation of the heat balance integral technique for slabs is covered by Goodman [2]. Basically, the technique is much the same as the momentum integral of fluid dynamics. The heat conduction equation is satisfied on the average by integrating it over the thickness of the body. A second-degree polynomial temperature profile is then assumed and the three arbitrary constants are evaluated from the boundary conditions. Substitution of this assumed profile into the integrated heat conduction equation leads for the case of the sphere to a second order, non-linear, ordinary differential equation in terms of the melt radius $r_s(t)$, and its first and second derivatives. The solution is easily obtained by numerical procedures.

Before integrating the heat conduction equation (3), the following transformation is made:

Let

$$u = Tr$$

Equation (3) then becomes (assuming constant thermal properties)

$$\frac{\partial u}{\partial t} = \kappa \frac{\partial^2 u}{\partial r^2} \quad ; \quad b < r < r_s \tag{12}$$

where $\kappa = \frac{k}{\rho c}$

and the conditions (4a to e) become

$$
\begin{aligned}
&\text{a)}\quad u(r,t_m) = u_o(r,t_m) \\
&\text{b)}\quad u(r_s,t) = r_s T_m \\
&\text{c)}\quad Q(t) = \frac{k}{r_s}\left[\left(\frac{\partial u}{\partial r}\right)_{r_s,t} - \frac{u(r_s,t)}{r_s}\right] - \rho L \frac{dr_s}{dt} \qquad (13) \\
&\text{d)}\quad \left(\frac{\partial u}{\partial r}\right)_{b,t} = \frac{u(b,t)}{b} \\
&\text{e)}\quad r_s(t_m) = a
\end{aligned}
$$

while the condition $\left(\frac{dr_s}{dt}\right)_{t_m} = 0$ remains unchanged. The integration of Eq. (12) over the thickness of the body yields

$$\int_b^{r_s} \frac{\partial u}{\partial t}\, dr = \kappa \int_b^{r_s} \frac{\partial^2 u}{\partial r^2}\, dr .$$

Upon letting:

$$G = \int_b^{r_s} u\, dr = \int_b^{r_s} Tr\, dr$$

it can readily be shown that

$$\frac{dG}{dt} - T_m r_s \frac{dr_s}{dt} = \kappa\left[\left(\frac{\partial u}{\partial r}\right)_{r_s,t} - \left(\frac{\partial u}{\partial r}\right)_{b,t}\right] . \qquad (14)$$

The substitution of Eqs. (13b,c and d) into Eq. (14) yields

$$\frac{dG}{dt} - T_m r_s \frac{dr_s}{dt} = \frac{\kappa r_s}{k}\left[Q + \rho L \frac{dr_s}{dt}\right] + \kappa T_m - \kappa T(b,t) . \qquad (15)$$

It is now assumed that the temperature $T(r,t)$ can be expressed at any time as a second order polynomial in $(r - b)$ with time dependent coefficients. That is,

$$T = A + B(r - b) + D(r - b)^2 \ .$$

Using conditions (4b,c and d), A, B, and D can be determined. The resulting temperature profile is

$$T = T_m - \left[\frac{Q + \rho L \frac{dr_s}{dt}}{2k}\right]\left[(r_s - b) - \frac{(r - b)^2}{(r_s - b)}\right] \qquad (16)$$

$$\text{for } r_s \neq b$$

Therefore, if the solution for r_s can be found, the temperature profile through the thickness of the body would be specified at any time by Eq. (16). G and T(b,t) can now be evaluated from Eq. (16) and the subsequent substitution into Eq. (15) yields

$$\frac{d^2 r_s}{dt^2} = -\left[\frac{Q}{\rho L} + \frac{dr_s}{dt}\right]\left\{\frac{(r_s - b)(9r_s + 7b)\frac{dr_s}{dt} + 12\kappa(3r_s - b)}{(r_s - b)^2(3r_s + 5b)}\right\} \qquad (17)$$

a second order, non-linear, ordinary differential equation for $r_s(t)$.

The numerical procedure used here for the solution of Eq. (17) follows that of Method I. For small $(t - t_m)$, $r_s(t)$ is expanded in a Taylor series about $t = t_m$. The first two coefficients of this series are determined from the conditions at $t = t_m$, and the third coefficient $\left(\frac{d^2 r_s}{dt^2}\right)_{t=t_m}$ is obtained by evaluating Eq. (17) at $t = t_m$. The remaining coefficients, $\left(\frac{d^3 r_s}{dt^3}\right)_{t=t_m}$, ... $\left(\frac{d^N r_s}{dt^N}\right)_{t=t_m}$ are obtained by successively differentiating Eq. (17) with respect to t and evaluating the results at $t = t_m$.

To determine $r_s(t_i + \Delta t)$ and $\frac{dr_s}{dt}(t_i + \Delta t)$ the following numerical scheme is used:

$$r_s(t_i + \Delta t) = r_s(t_i) + \Delta t \frac{dr_s}{dt}(t_i)$$

$$\frac{dr_s}{dt}(t_i + \Delta t) = \frac{dr_s}{dt}(t_i) + \Delta t \frac{d^2 r_s}{dt^2}(t_i)$$

and $\frac{d^2 r_s}{dt^2}(t_i + \Delta t)$ is determined from Eq. (17).

Numerical Calculations

Calculations using both Methods I (Citron) and II (Goodman) are performed for a one inch thick 7-3/4 inch outside diameter aluminum sphere under a constant radial heat flux* and average constant thermal and physical properties (Table I). Two values of σ_o (=ha/k=0.70, 1.10), the non-dimensional surface heat transfer coefficient, and a stagnation temperature of 1850°R, are used in the analysis. These values were chosen on the basis of typical heat inputs to re-entry vehicles.

The pre-melt solution for the temperature is obtained through the use of the one-dimensional solutions in Ref. [17]. The outer surface temperature-time histories as well as the times at which melting first occurs are shown in Fig. 1. The corresponding temperature distributions at the melt time are given in Fig. 2. The melt analysis of Methods I and II are then used to proceed.

Method I:

A six term Taylor series expansion for $\theta(Z,\tau)$ is assumed. The substitution of this expansion into Eq. (11) yields a non-linear, ordinary, differential equation containing up to the third order time derivatives of R_s. It should be noted that the highest order derivative ($\dddot{R}_s$) appears linearly in this equation. As previously mentioned, this necessitates the matching of $\theta(Z,0)$ with the pre-melt solution (at $\tau = 0$) at $K-2$ points. In this case, therefore, only one match point is necessary. The point chosen is at the insulated surface ($r = b$). This enables the evaluation of $\ddot{R}_s(0)$, while $\dddot{R}_s(0)$ is found from Eq. (11). The

*Since the surface temperature is assumed to remain at melt temperature during the melt analysis, a constant heat flux corresponds to steady-state aerodynamic heating during melting.

numerical procedure previously discussed is then used to obtain R_s as a function of τ. Figures 3 and 4 illustrate the values of melt depth versus time. It should be noted that the solution for $r_s(t)$ rapidly approaches a steady state; that is, $\frac{dr_s}{dt}$ approaches a constant value. This is not unexpected since at $t = t_m$, the pre-melt analysis yields a temperature profile through the thickness which is almost at the constant melt temperature. Therefore, from the boundary condition on the heat input [Eq. (4c)],

$$Q \longrightarrow -\rho L \frac{dr_s}{dt} ,$$

and since in this analysis it is assumed $Q = \text{constant}$,

$$\frac{dr_s}{dt} \longrightarrow -\frac{Q}{\rho L} \quad ; \quad \text{a constant} .$$

This condition is indeed rapidly approached as shown in Figs. 3 and 4.

The Taylor series expansion Eq. (10) can now be used to determine $\theta(Z,\tau)$ versus Z for a specific τ. Figs. 5 and 6 show temperature profiles for times greater than the melt time, while Fig. 2 presents the results at the melt time.

Method II:

The numerical procedure previously discussed is applied to Eq. (17). The resulting numerical values for the melt depth are presented in Figs. 3 and 4. Equation (16) is then used to calculate the temperature profiles at the melt time (Fig. 2) and at times greater than the melt time (Figs. 5 and 6).

Conclusions

The purpose of this report was to obtain the one-dimensional ablation characteristics of a hollow sphere by adapting the Taylor series expansion technique (Method I) originally developed for a slab by Citron [1], and also by using Goodman's [2] heat balance technique (Method II). Because of the relative simplicity of the numerical procedures of Method II, it was deemed appropriate to obtain solutions using this heat balance technique and to compare these to the more exact solutions determined from Method I.

A six-term Taylor series expansion was used in Method I. It was necessary to include this number of terms in order to approximate the temperature profile at the melt time with sufficient accuracy. A quadratic temperature profile for all time was used in Method II and the comparison indicates that the predicted profile is in good agreement with both the exact premelt solution and the solution obtained from Method I (Fig. 2).

In obtaining a solution by using Method I (six-term expansion), however, it was necessary to use the insulated surface temperature at the melt time. Hence, the exact solution for the temperature profile is approximated more closely by Method I than by Method II (Fig. 2). This also accounts for the differences between the temperature profiles shown in Figs. 5 and 6.

The melt depths predicted by both methods, however, are in excellent agreement (Figs. 3 and 4). Furthermore, as shown in Figs. 3 and 4, the rate of ablation rapidly approaches a constant value. This is not surprising since, as shown in Figs. 2, 5 and 6, a constant temperature distribution is also rapidly approached.

In conclusion, it is clearly seen that the numerically simpler technique (Method II) can be applied to the ablating sphere and yields results which are quite close to those obtained using the more complex technique (Method I). Both of these methods predict ablation profiles which are almost identical. It is apparent that future investigations should include both the two-dimensional effects and the effects of variation of the material thermal properties with temperature.

References

1. Citron, S.J.: On the Conduction of Heat in a Melting Slab. Columbia University, Department of Civil Engineering and Engineering Mechanics, Technical Report No. 18, March 1961.

2. Goodman, T.R.: The Heat Balance Integral and its Application to Problems Involving a Change of Phase. 1957 Heat Transfer and Fluid Mechanics Institute, pp. 383-400, June 1957.

3. Landau, H.G.: Heat Conduction in a Melting Solid. Quarterly of Applied Mathematics, Vol. 8, pp. 81-94, April 1950.

4. Lotkin, M.: The Calculation of Heat Flow in Melting Solids. Quarterly of Appl. Math., Vol. 18, No. 1, pp. 79-85, April 1960.

5. Ehrlich, L.W.: A Numerical Method of Solving a Heat Flow Problem with Moving Boundary. Journal of the Association for Computing Machinery, Vol. 5, No. 2, pp. 161-176, April 1958.

6. Dewey, K.F., Schlesinger, S.I., and Sashkin, L.: Temperature Profiles in a Finite Solid with Moving Boundary. Journal of the Aero/Space Sciences, Vol. 27, No. 1, pp. 59-64, January 1960.

7. Goodman, T.R.: Aerodynamic Ablation of Melting Bodies. Proceedings of the Third U.S. National Congress of Applied Mechanics, pp. 735-745, 1958.

8. Adams, Mac C.: Recent Advances in Ablation. American Rocket Society Journal, Vol. 29, pp. 625-632, September 1959.

9. Carslaw, H.S. and Jaeger, J.C.: Conduction of Heat in Solids. Clarendon Press, Oxford, Second Edition, 1959.

10. Citron, S.J.: Heat Conduction in a Melting Slab. Journal of the Aero/Space Sciences, Vol. 27, No. 3, March 1960.

11. Boley, B.A.: A Method of Heat Conduction Analysis of Melting and Solidification Problems. Journal of Mathematics and Physics, Vol. 40, No. 4, pp. 300-313, December 1961.

12. Swann, R.T. and South, J.: A Theoretical Analysis of Effects of Ablation on Heat Transfer to an Arbitrary Axisymmetric Body. NASA TN D-741, April 1961.

13. Lew, H.G. and Fanucci, J.B.: A Study of Melting Surfaces. Aerophysics Research Memo 38, General Electric Report R59SD381, April 1959.

14. Fleddermann, R.G. and Hurwicz, H.: Transient Ablation and Heat Conduction Phenomena at a Vaporizing Surface. Research and Advanced Development Division, AVCO Corporation, Technical Report RAD-TR-9(7)-60-9, April 1960.

15. Sutton, G.W.: The Hydrodynamics and Heat Conduction of a Melting Solid. Journal of Aeronautical Sciences, Vol. 25, pp. 29-32, 36, January 1958.

16. Economos, C.: Results of Ablation Tests on Several Plastic Models in a Hypersonic Wind Tunnel. Polytechnic Institute of Brooklyn, PIBAL Report No. 606, WADD TN 60-273, March 1961.

17. Smithson, R.E. and Thorne, C.J.: Temperature Tables. U.S. Naval Ordnance Test Station, NAVORD Report 5562, Part 6, NOTS 2088, September 1958.

TABLE I

Average Thermal and Physical Properties of 356-T6 Cast Aluminum Alloy

c	0.245 $\frac{BTU}{lb\,^{o}R}$
k	0.33 $\frac{BTU\ IN}{ft^{2}\ sec\,^{o}R}$
L	128 $\frac{BTU}{lb}$
T_m	1590 ^{o}R
κ	0.0951 $\frac{in^{2}}{sec}$
ρ	170 $\frac{lb}{ft^{3}}$

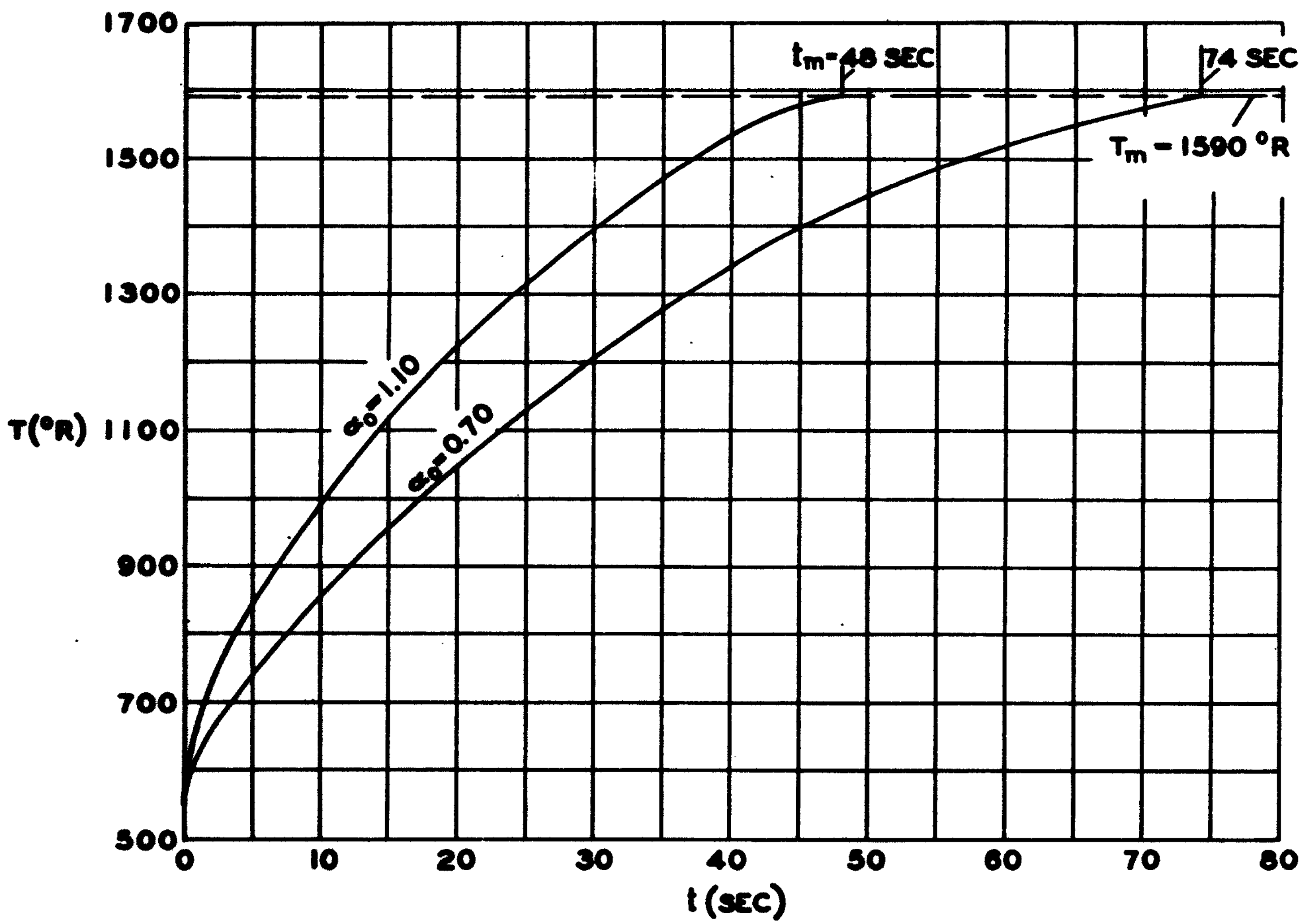

FIG. 1 HEATED SURFACE TEMPERATURE DISTRIBUTIONS

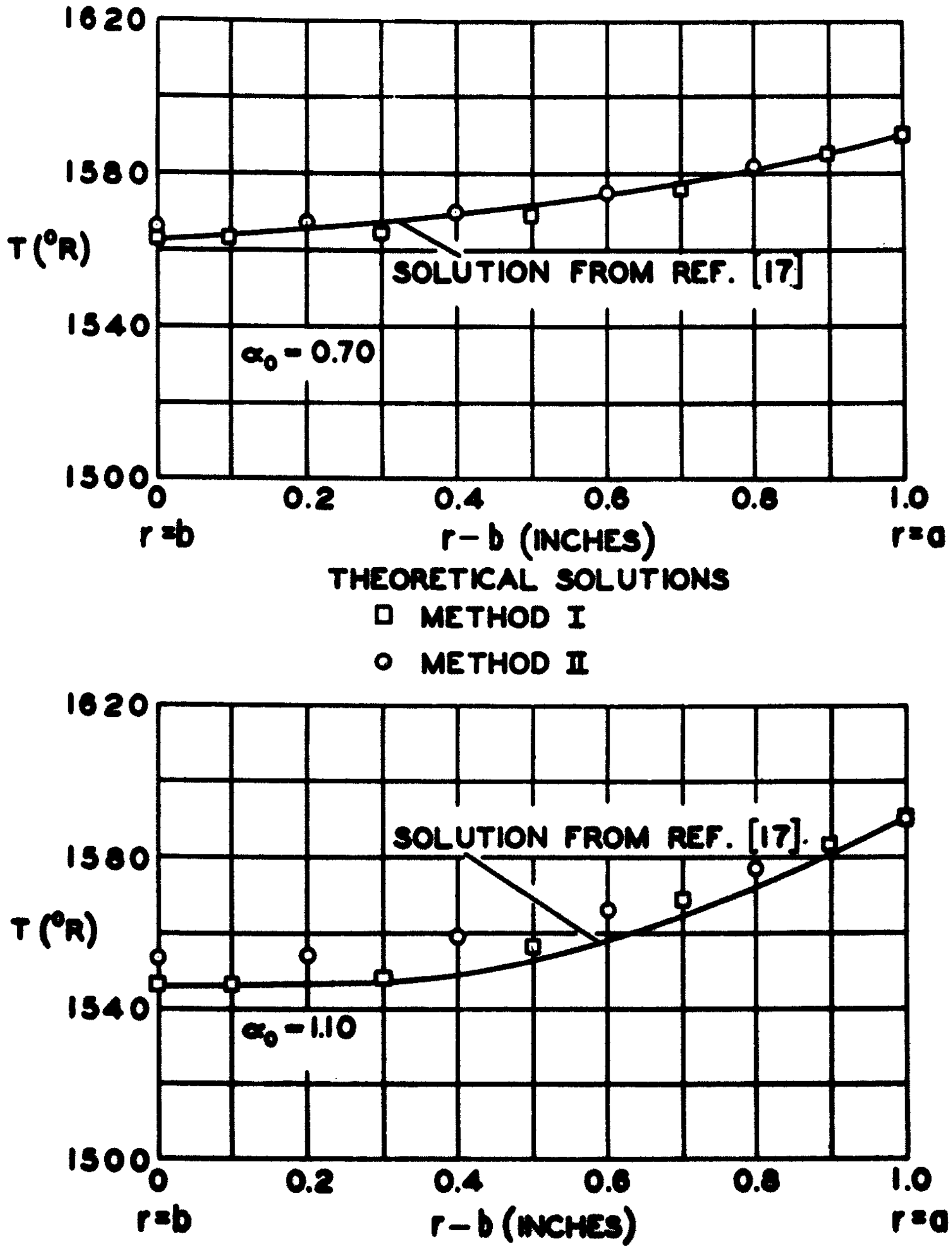

FIG. 2
TEMPERATURE PROFILES AT MELT TIME $(t = t_m)$

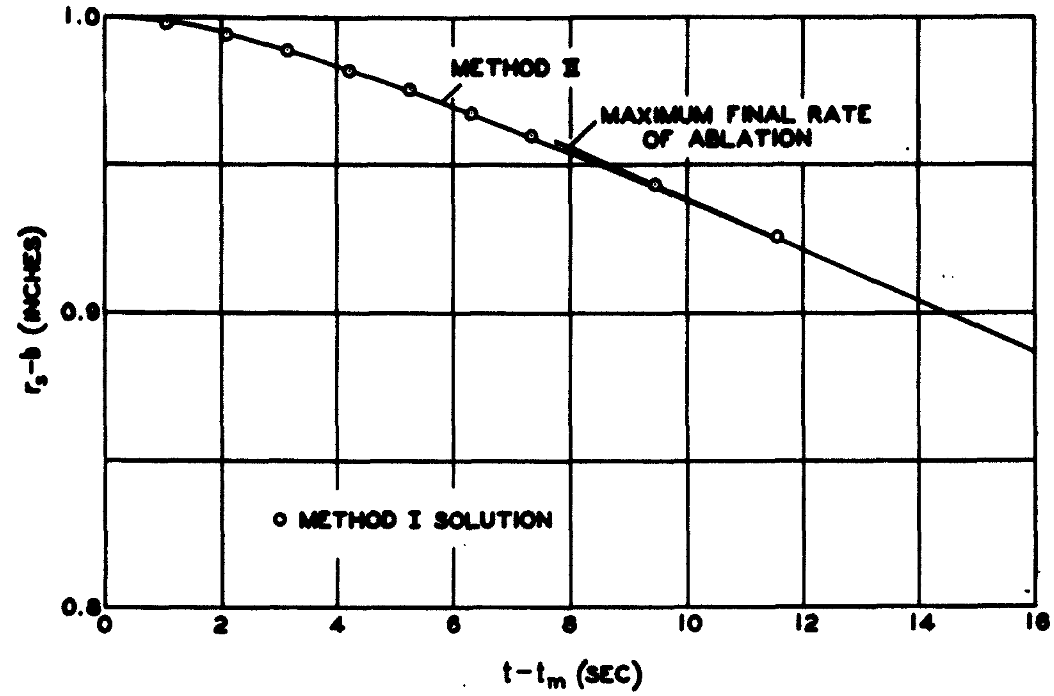

FIG. 3 ABLATION DEPTH VERSUS TIME FOR $\alpha_0 = 0.70$

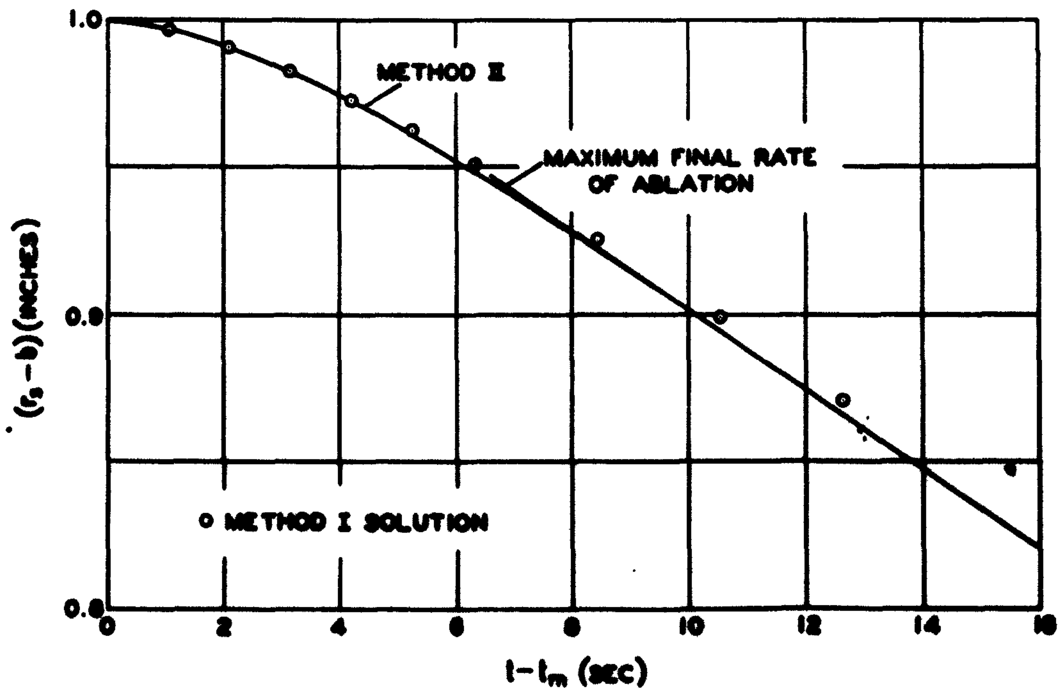

FIG. 4 ABLATION DEPTH VERSUS TIME FOR $\alpha_0 = 1.10$

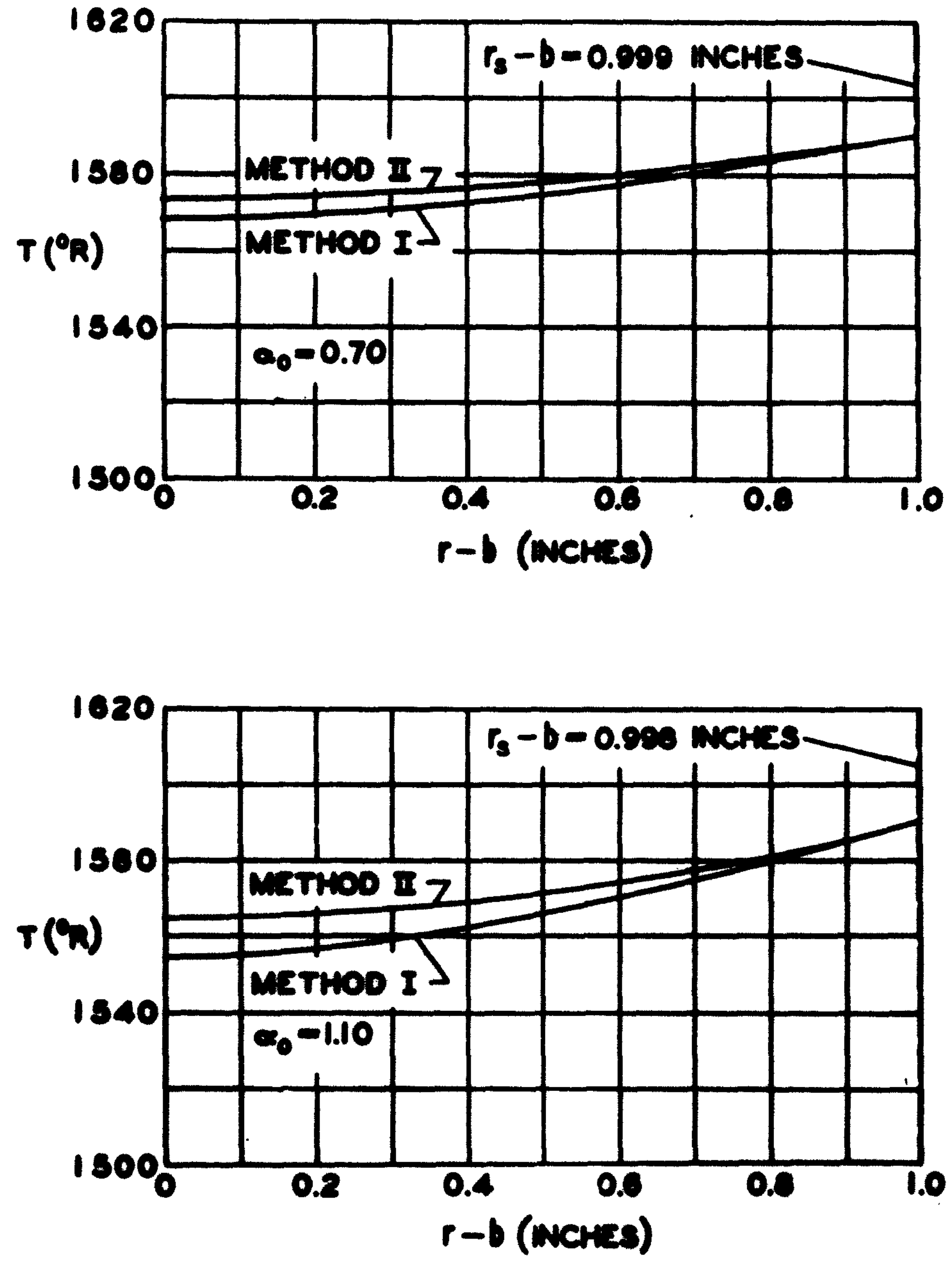

FIG. 5 TEMPERATURE PROFILES AT $t - t_m = 1$ SEC.

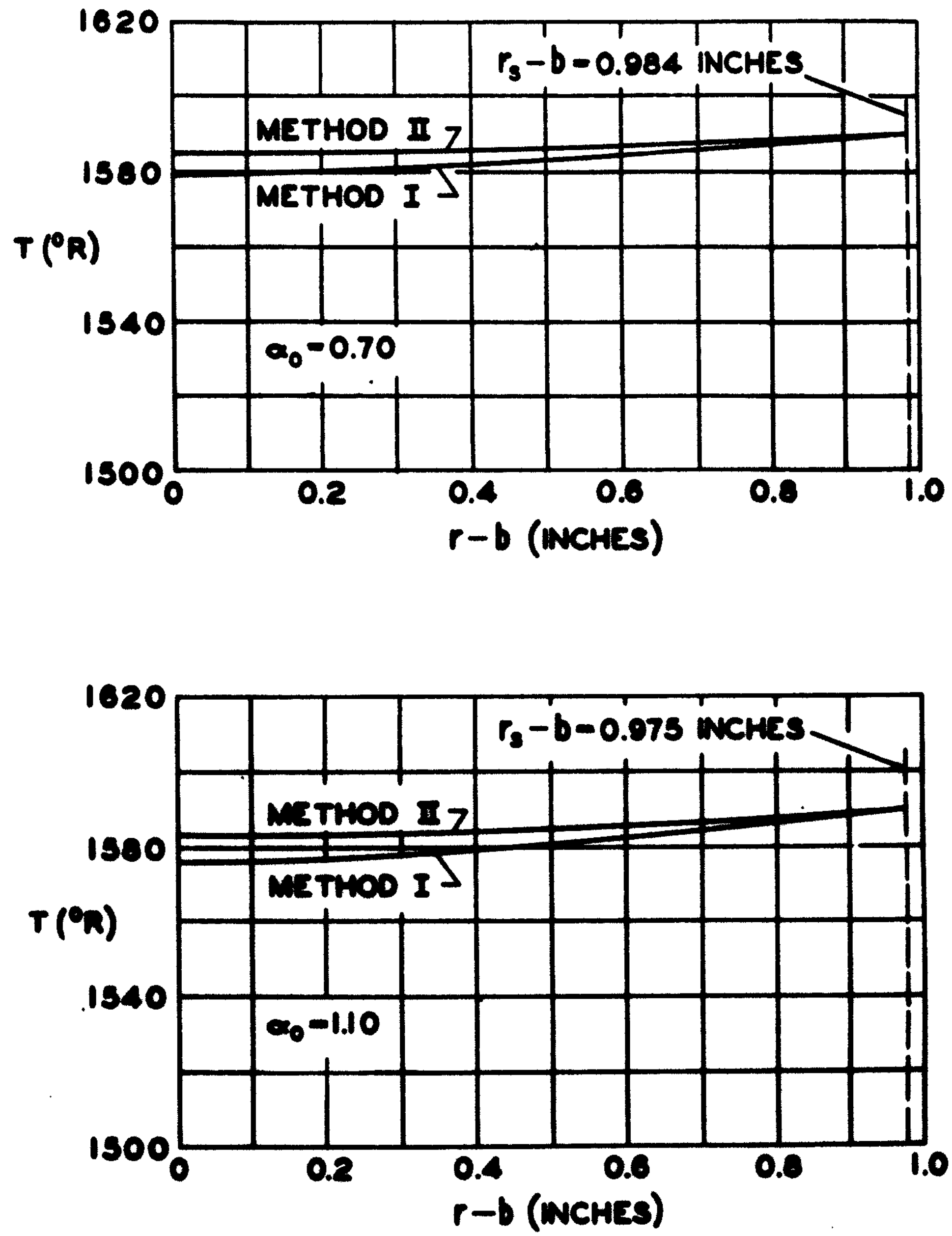

FIG. 6 TEMPERATURE PROFILES AT $t - t_m = 4$ SEC.

DISTRIBUTION LIST FOR UNCLASSIFIED
TECHNICAL REPORTS ISSUED UNDER
CONTRACT NONR 839(23), TASK NR 064-433

Chief of Naval Research
Department of the Navy
Washington 25, D.C.
Attn: Code 438

Commanding Officer
Office of Naval Research
Branch Office
495 Summer Street
Boston 10, Mass. (1)

Commanding Officer
Office of Naval Research
Branch Office
John Crerar Library Building
86 E. Randolph Street
Chicago 11, Illinois (1)

Commanding Officer
Office of Naval Research
Branch Office
346 Broadway
New York 13, N.Y. (1)

Commanding Officer
Office of Naval Research
Branch Office
1030 E. Green Street
Pasadena, California (1)

Commanding Officer
Office of Naval Research
Branch Office
1000 Geary Street
San Francisco, California (1)

Commanding Officer
Office of Naval Research
Navy No. 100, Fleet Post Office
New York, N.Y. (25)

Director
Naval Research Laboratory
Washington 25, D.C.
Attn: Tech. Info. Officer (6)
Code 6200 (1)
Code 6205 (1)
Code 6250 (1)
Code 6260 (1)

Armed Services Technical Info. Agency
Arlington Hall Station
Arlington 12, Va. (10)

Office of Technical Services
Department of Commerce
Washington 25, D.C. (1)

Office of the Secretary of Defense
Research and Development Div.
The Pentagon
Washington 25, D.C.
Attn: Technical Library (1)

Chief
Defense Atomic Support Agency
Washington 25, D.C.
Attn: Doc. Libr. Br. (1)

Office of the Secretary of the Army
The Pentagon
Washington 25, D.C.
Attn: Army Library (1)

Chief of Staff
Department of the Army
Washington 25, D.C.
Attn: Develop. Br. (R and D Div.) (1)
Research Branch (R and D Div) (1)
Spec. Weapons Br. (R and D Div) (1)

Office of the Chief of Engineers
Department of the Army
Washington225, D. C.
Attn: ENG-EB Prot. Constr. Br., Eng. Div. Mil. Constr. (1)
ENG HL Lib. Br. Adm. Ser. Div. (1)
ENG EA Struc. Br., Eng. Div. Mil. Constr. (1)
ENG NB Special Eng. Br. Eng. R & D Di.v (1)
ENG WD Planning Div. Civil Works (1)

Commanding Officer
Engineer Research Development Lab.
Fort Belvoir, Virginia (1)

Office of the Chief of Ordnance
Department of the Army
Washington 25, D. C.
Attn: Research & Materials Branch (Ord. R & D DIV.) (1)

Commanding Officer
Watertown Arsenal
Watertown, Massachusetts
Attn: Laboratory Division (1)

Commanding Officer
Frankford Arseanl
Bridesburg Station
Philadelphia 37, Pennsylvania
Attn: Laboratory Division (1)

Office of Ordnance Research
2127 Myrtle Drive
Duke Station
Durham, North Carolina
Attn: Division of Engineering Scis. (1)

Commanding Officer
U.S. Army Signal Research & Develop. Lab.
SIGFM/EL-G
Fort Monmouth, New Jersey (1)

Chief of Naval Operations
Department of the Navy
Washington 25, D.C.
Attn: Op 37 (1)

Commandant, Marine Corps
Headquarters, US. Marine Corps
Washington 25, D.C. (1)

Chief, Bureau of Ships
Department of the Navy
Washington 225, D. C.
Attn: Code 312 (2)
Code 376 (1)
Code 377 (1)
Code 420 (1)
Code 423 (2)
Code 442 (2)

Chief, Bureau of Aeronautics
Deparment of the Navy
Washington 25, D. C.
Attn: AE-4 (1)
AV-34 (1)
AD (1)
AD-2 (1)
RS-7 (1)
RS-8 (1)
SI (1)
TS-42 (1)

Chief Bureau of Ordnance
Department of the Navy
Washington 25, D.C.
Attn: Ad3 (1)
Re (1)
Res (1)
Reu (1)
Re85 (1)
Re81 (1)
Ren (1)

Special Projects Office
Bureau of Ordnance
Department of the Navy
Washington 25, D.C.
Attn: Missile Branch (2)

Chief, Bureau of Yards & Docks
Department of the Navy
Washington 25, D. C.
Attn: Code D-202 (1)
Code D-202.3 (1)
Code D-220 (1)
Code D-222 (1)
Code D-410C (1)
Code D-440 (1)
Code D-500 (1)

Commanding Officer & Director
David Taylor Model Basin
Washington 7, D.C.
Attn: Code 140 (1)
Code 600 (1)
Code 700 (1)
Code 720 (1)
Code 725 (1)
Code 731 (1)
Code 740 (2)

Commander
U.S. Naval Ordnance Laboratory
White Oak, Maryland
Attn: Technical Library (2)
Technical Evaluation Department (1)

Director
Materials Laboratory
New York Naval Shipyard
Brooklyn 1, New York (1)

Commanding Officer & Director
U.S. Naval Electronics Laboratory
San Diego 52, California (1)

Officer-in-Charge
Naval Civil Engineering Research & Evaluation Laboratory
U.S. Naval Construction Battalion Center
Port Hueneme, California (2)

Director
Naval Air Experimental Station
Naval Air Material Center
Naval Base
Philadelphia 12, Pennsylvania
Attn: Materials Laboratory (1)
Structures Laboratory (1)

Officer-in-Charge
Underwater Explosion Research Division
Norfolk Naval Shipyard
Portsmouth, Virginia
Attn: Dr. A. H. Keil (2)

Commander
U.S. Naval Proving Grounds
Dahlgren, Virginia (1)

Commander
Naval Ordnance Test Station
Inyokern, China Lake, California
Attn: Physics Division (1)
Mechanics Branch (1)

Commander
Naval Ordnance Test Station
Underwater Ordnance Division
3202 E. Foothill Boulevard
Pasadena 8, California
Attn: Structures Division (1)

Commanding Officer & Director
Naval Engineering Experiment Station
Annapolis, Maryland (1)

Superintendent
Naval Post Graduate School
Monterey, California (1)

Commandant Marine Corps Schools
Quantico, Virginia
Attn: Director, Marine Corps Development Center (1)

Commanding General
U. S. Air Force
Washington 25, D.C.
Attn: Research & Develonment Division (1)

Commander
Air Material Command
Wright-Patterson Air Force Base
Dayton, Ohio
Attn: MCREX-B (1)
Structures Division (1)

Commander
U.S. Air Force Institute
of Technology
Wright-Patterson Air Force Base
Dayton, Ohio
Attn: Chief, Applied Mechanics
Group (1)

Director of Intelligence
Headquarters, U.S. Air Force
Washington 25, D.C.
Attn: P.V. Branch
(Air Targets Div.) (1)

Commander
Air Force Office of Scientific
Research
Washington 25, D.C.
Attn: Mechanics Divsion (1)

U.S. Atomic Energy Commission
Washington 25, D.C.
Attn: Director of Research (2)

Director
National Bureau of Standards
Washington 25, D.C.
Attn: Division of Mechanics (1)
Engineering Mechanics
Section (1)
Aircraft Structures (1)

Commandant
U.S. Coast Guard
1300 E Street, N.W.
Washington 25, D.C.
Attn: Chief, Testing & Devel.
Div. (1)

U.S. Maritime Administration
General Administration Office
Building
Washington 25, D.C.
Attn: Chief, Div. of Preliminary
Design (1)

National Aeronautics & Space
Administration
1512 H Street, N.W.
Washington 25, D.C.
Attn: Loads & Structures Div. (2)

Director
Langley Aeronautical Laboratory
Langley Field, Virginia
Attn: Structures Division (2)

Director
Forest Products Laboratory
Madison, Wisconsin (1)

Civil Aeronautics Administration
Department of Commerce
Washington 25, D.C.
Attn: Chief, Aircraft Engineering
Div. (1)
Chief, Airframe & Equipment
Branch (1)

National Sciences Foundation
1520 H Street, N.W.
Washington, D.C.
Attn: Engineering Sciences Div. (1)

National Academy of Sciences
2101 Constitution Avenue
Washington 25, D.C.
Attn: Technical Director, Comm. on
Ships' Structural Design (1)
Exec. Sec'y, Comm. on Under-
sea Warfare (1)

Professor Lynn S. Beedle
Fritz Engineering Laboratory
Lehigh University
Bethlehem, Pa. (1)

Professor R.L. Bisplinghoff
Dept. of Aeronautical Engrg.
Mass. Institute of Technology
Cambridge 39, Mass. (1)

Professor H.H. Bleich
Dept. of Civil Engineering
Columbia University
New York 27, New York (1)

Professor B.A. Boley
Dept. of Civil Engineering
Columbia University
New York 27, New York (1)

Professor G. F. Carrier
Pierce Hall
Harvard University
Cambridge 38, Massachusetts (1)

Professor Herbert Deresiewicz
Department of Civil Engineering
Columbia University
632 W. 125th Street
New York 27, New York (1)

Professor D. C. Drucker, Chairman
Division of Engineering
Brown University
Providence 12, Rhode Island (1)

Professor A. C. Eringen
Department of Aeronautical Engineering
Purdue University
Lafayette, Indiana (1)

Professor W. Flugge
Department of Mechanical Engineering
Stanford University
Stanford, California (1)

Professor J. N. Goodier
Department of Mechanical Engineering
Stanford University
Stanford, California (1)

Professor L. E. Goodman
Engineering Experiment Station
University of Minnesota
Minneapolis, Minnesota (1)

Professor M. Hetenyi
The Technological Institute
Northwestern University
Evanston, Illinois (1)

Professor P. G. Hodge, Jr.
Department of Mechanics
Technology Center
Illinois Inst. of Technology
Chicago 16, Illinois (1)

Professor N.J. Hoff, Head
Division of Aeronautical Engineering
Stanford University
Stanford, California (1)

Professor W. H. Hoppmann, II
Department of Mechanics
Rensselaer Polytechnic Institute
Troy, New York (1)

Professor Bruce G. Johnston
University of Michigan
Ann Arbor, Michigan (1)

Professor J. Kempner
Department of Aeronautical Engineering
and Applied Mechanics
Polytechnic Institute of Brooklyn
333 Jay Street
Brooklyn 1, New York (1)

Professor H. L. Langhaar
Department of Theoretical and Applied
Mechanics
University of Illinois
Urbana, Illinois (1)

Professor B. J. Lazan, Director
Engineering Experiment Station
University of Minnesota
Minneapolis 14, Minnesota (1)

Professor E. H. Lee
Division of Applied Mathematics
Brown University
Providence 12, Rhode Island (1)

Professor George H. Lee
Director of Research
Rensselaer Polytechnic Institute
Troy, New York (1)

Mr. M. M. Lemcoe
Southwest Research Institute
8500 Culebra Road
San Antonio 6, Texas (1)

Professor Paul Lieber
Geology Department
University of California
Berkeley 4, California (1)

Professor R.D. Mindlin
Department of Civil Engineering
Columbia University
632 W. 125th Street
New York 27, New York (1)

Professor Paul M. Naghdi
Building T-7
College of Engineering
University of California
Berkeley 4, California (1)

Professor William A. Nash
Department of Engineering
Mechanics
University of Florida
Gainesville, Florida (1)

Professor N.M. Newmark, Head
Department of Civil Engineering
University of Illinois
Urbana, Illinois (1)

Professor Aris Phillips
Department of Civil Engineering
15 Prospect Street
Yale University
New Haven, Connecticut (1)

Professor W. Prager, Chairman
Physical Sciences Council
Brown University
Providence 12, Rhode Island (1)

Professor E. Reissner
Department of Mathematics
Massachusetts Institute of
Technology
Cambridge 39, Massachusetts (1)

Professor M.A. Sadowsky
Department of Mechanics
Rensselaer Polytechnic Institute
Troy, New York (1)

Professor J. Stallmeyer
Department of Civil Engineering
University of Illinois
Urbana, Illinois (1)

Professor Eli Sternberg
Department of Mechanics
Brown University
Providence 12, Rhode Island (1)

Professor S.P. Timoshenko
School of Engineering
Stanford University
Stanford, California (1)

Professor A.S. Velestos
Department of Civil Engineering
University of Illinois
Urbana, Illinois (1)

Professor Dana Young
Yale University
New Haven, Connecticut (1)

Project Staff (10)

For your future distribution (10)

Dr. John F. Brahtz
Department of Engineering
University of California
Los Angeles, California (1)

Mr. Martin Goland, Vice President
Southwest Research Institute
8500 Culebra Road
San Antonio, Texas (1)

Mr. S. Levy
General Electric Research Laboratory
6901 Elmwood Avenue
Philadelphia 42, Pennsylvania (1)

Professor B. Budiansky
Department of Mechanical
Engineering
School of Applied Sciences
Harvard University
Cambridge 38, Massachusetts (1)

Professor H. Kolsky
Division of Engineering
Brown University
Providence 12, Rhode Island (1)

Professor E. Orowan
Department of Mechanical
Engineering
Massachusetts Institute of Technology
Cambridge 39, Massachusetts (1)

Professor J. Ericksen
Mechanical Engineering Department
Johns Hopkins University
Baltimore 18, Maryland (1)

Professor T. Y. Thomas
Graduate Institute for
Mathematics and Mechanics
Indiana University
Bloomington, Indiana (1)

Professor Joseph Martin, Head
Department of Engineering Mechanics
College of Engineering and Architecture
Pennsylvania State University
University Park, Pennsylvania (1)

Mr. K. H. Koopman, Secretary
Welding Research Council of
The Engineering Foundation
29 West 39th Street
New York 18, New York (2)

Professor Walter T. Daniels
School of Engineering & Architecture
Howard University
Washington 1, D. C. (1)

Dr. D. O. Brush
Structures Department 53-13
Lockheed Aircraft Corporation
Missile Systems Division
Sunnyvale, California (1)

Professor Nicholas Perrone
Engineering Science Department
Pratt Institute
Brooklyn 5, New York (1)

Cambridge Acoustical Association
129 Mount Auburn Street
Cambridge 39, Massachusetts (1)

Legislative Reference Service
Library of Congress
Washington 25, D. C.
Attn: Dr. E. Wenk (1)

Commanding Officer
USNNOEU
Kirtland Air Force Base
Albuquerque, New Mexico
Attn: Code 20
(Dr. J. N. Brennan (1)

Professor J. E. Cermak
Department of Civil Engineering
Colorado State University
Fort Collins, Colorado (1)

Professor W. J. Hall
Department of Civil Engineering
University of Illinois
Urbana, Illinois (1)

Professor R. P. Harrington, Head
Department of Aeronautical Engineering
University of Cincinnati
Cincinnati 21, Ohio (1)

Professor Eugene J. Brunelle, Jr.
Department of Aeronautical Engineering
Princeton University
Princeton, New Jersey (1)

Commander
WADD
Wright-Patterson Air Force Base
Ohio
Attn: WWRC (1)
WWRMDD (1)
WWRCDS (1)